Two-dimensional Vortex-induced Vibrations of Submerged Floating Tunnel Tethers

F. Ge, X. Long, L. Wang, Y. Hong
State Key Laboratory of Nonlinear Mechanics, Institute of Mechanics, Chinese Academy of Sciences, Beijing, China

ABSTRACT: A vortex−induced vibration (VIV) model is presented for predicting the nonlinear dynamic response of submerged floating tunnel (SFT) tethers which are subjected to wave, current and tunnel oscillatory displacements at their upper end in horizontal and vertical directions. A nonlinear fluid force formula is introduced in this model, and the effect of the nonlinearity of tether is investigated. First, the tunnel is stationary and the tether vibrates due to the vortices shedding. The calculated results show that the cross-flow amplitude of VIV decreases compared with the linear model. However the in−line amplitude of VIV increases. Next, the periodical oscillation of tunnel is considered. The oscillation caused by wave forces plays the roles of parametric exciter and forcing exciter to the VIV of tether. The time history of displacement of the tether mid-span is obtained by the proposed model. It is shown that the in−line amplitude increases obviously and the corresponding frequency is changed. The cross-flow amplitude exhibits a periodic behavior.

1 INTRODUCTION

A submerged floating tunnel (SFT) can be an alternative structure to rock tunnels below the sea bottom or long span bridges above the surface. The SFT technique offers the opportunity to plan crossings where they have never before been thought possible. In other cases, SFT may be an alternative to another type of fixed crossings, such as bridge, floating bridge, bored tunnel, or immersed tunnel. One of the advantages of SFT is that the crossing may be invisible from the surface, making it attractive from an environmental standpoint. In addition, the surface waterway traffic is not obstructed (Ahrens 1997). However, up to now, there is not a real SFT being constructed in the world. One of the most essential obstacles in the realization of SFT is its dynamic behaviour in water environment, which is not well understood (Huang et al. 2002).

If the weight of SFT is smaller than its buoyancy, the tunnel is necessary to be moored to the waterbed by tethers just shown as Figure 1. In an ocean environment, the tethers are subjected to wave, current and tunnel oscillations at their upper ends. The stability of the tether is crucial to the safety of entire tunnel, but the tether may fail due to relevant vortex-induced vibration.

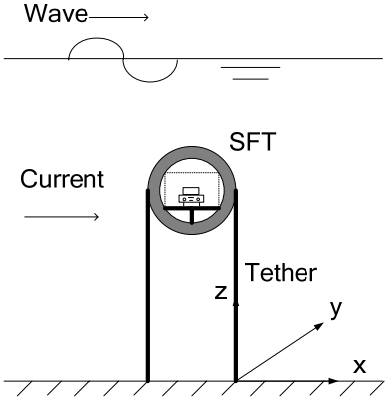

Figure 1. Schematic diagram and coordinate system.

Brancaleoni et al.(1989) developed an engineering analysis program for the behaviour of SFT under wave or seismic condition. Remseth et al. (1999) investigated the dynamic response of SFT using finite element method. The hydrodynamic analysis was based on Navier-Stokes equation. Kunisu et al.(1994) presented the response of SFT due to wave forces through model tests. Mai et al. (2004) considered the influence of tether tension on the VIV of tether. Most of the literature available is

on the VIV of tether in cross-flow direction and the influence of the oscillation of tunnel has never been considered. The present study attempt to investigate the VIV of tether in the presence of external excitations which include the parametric excitation and forcing excitation induced by the oscillation of tunnel.

2 MODEL FORMULATION

A Cartesian right-hand coordinate system is defined with x and y in the horizontal plane and z vertically upwards(Figure 1). Considering a tether with uniform material properties and constant diameter D, which follows the z axis and is pinned at two ends, the dynamic equations can be expressed as

$$\begin{cases} \bar{m}\dfrac{\partial^2 x}{\partial t^2}+(C+C')\dfrac{\partial x}{\partial t}+EI\dfrac{\partial^4 x}{\partial z^4}-T\dfrac{\partial^2 x}{\partial z^2}=F_{\mathrm{x}} \\ \bar{m}\dfrac{\partial^2 y}{\partial t^2}+(C+C')\dfrac{\partial y}{\partial t}+EI\dfrac{\partial^4 y}{\partial z^4}-T\dfrac{\partial^2 y}{\partial z^2}=F_{\mathrm{y}} \end{cases} \tag{1}$$

where $\bar{m}$ is the total mass per unit length including added mass, C is the damping coefficient, C' is the linearized fluid damping coefficient which is relevant to the vortex shedding frequency ω_s and is given by Facchinetti et al.(2004)

$$C'=\gamma\omega_s\rho D^2 \tag{2}$$

where, γ is a parameter determined through experiment and is equal to 0.8, ρ is fluid density and D is the outer diameter of tether. In Equation (1), EI is the bending stiffness, T is the axial tension in the tether. F_{x} and F_{y} are the external hydrodynamic forces due to the wake dynamics.

For a stationary tether, the drag and lift forces coincide with the x and y axis, respectively, as shown in Figure 2(a). However, when the tether is vibrating as a result of vortex shedding, the drag and lift forces do not coincide with the x and y axis any more, which is shown in Figure 2(b) (Wang et al. 2003). The corresponding forces exerted on the tether can thus be expressed as

$$\begin{aligned} F_{\mathrm{x}} &= f_{\mathrm{D}}+f_{\mathrm{D}}'\cos\theta-f_L\sin\theta \\ F_{\mathrm{y}} &= f_{\mathrm{L}}\cos\theta+f_{\mathrm{D}}'\sin\theta \end{aligned} \tag{3}$$

where f_{D} is the average drag force, f_{D}', f_{L} is the vortex induced drag and lift force, respectivly, and θ is the angle between x axis and the instantaneous velocity of the tether, which is given by

$$\theta(t)=arctg\left(\frac{\dot{y}(t)}{U_{\mathrm{c}}-\dot{x}(t)}\right)=arctg\left(\frac{\dot{Y}(t)}{1-\dot{X}(t)}\right) \tag{4}$$

where the dot denotes differentiation with respect to time, $\dot{X}$, $\dot{Y}$ is the dimensionless velocity in x and y direction, respectively. Since, in general, $\dot{X}$ and $\dot{Y}$ are smaller than 1, the angle θ is very small and

$$\begin{aligned} \sin\theta(t) &= \frac{\dot{Y}(t)}{\sqrt{\dot{Y}^2(t)+\left(1-\dot{X}(t)\right)^2}}\approx\dot{Y}(t) \\ \cos\theta(t) &= \frac{1-\dot{X}(t)}{\sqrt{\dot{Y}^2(t)+\left(1-\dot{X}(t)\right)^2}}\approx 1 \end{aligned} \tag{5}$$

Substituting Equation (5) into Equation (3), we get the formulation of the right-hand side for Equation (1).

$$\begin{cases} F_{\mathrm{x}} = f_{\mathrm{D}}+f_{\mathrm{D}}'-f_{\mathrm{L}}\dot{Y}(t) \\ F_{\mathrm{y}} = f_{\mathrm{L}}+f_{\mathrm{D}}'\dot{Y}(t) \end{cases} \tag{6}$$

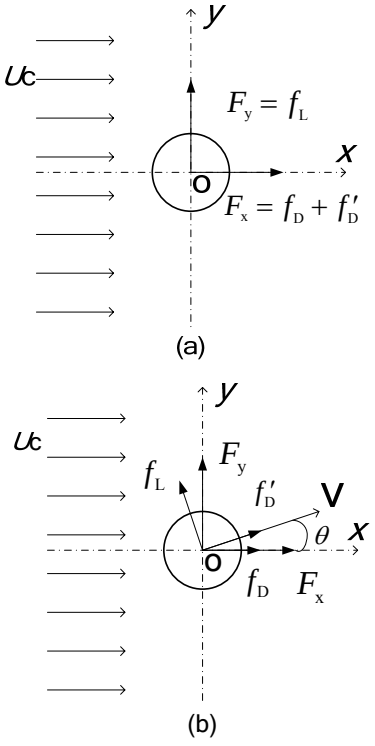

Figure 2. Illustration of the cross-section of tether in a cross flow and the fluid forces exerted on it: (a) stationary tether, (b) vibrating tether.

When lock-in occurs, the lift and drag forces per unit length can be simplified to be sinusoidal at the vortex shedding frequency ω_s and at $2\omega_s$, respectively, thus, they can be written as

$$\begin{aligned} f_{\mathrm{D}}(t) &= 1/2\,\bar{C}_{\mathrm{D}}\rho DU_{\mathrm{C}}^2 \\ f_{\mathrm{D}}'(t) &= 1/2\left(C_{\mathrm{D}}'\sin\left(2\omega_s t+\phi_{\mathrm{D}}\right)\right)\rho DU_{\mathrm{C}}^2 \\ f_{\mathrm{L}}(t) &= 1/2\left(C_{\mathrm{L}}\sin\left(\omega_s t+\phi_{\mathrm{L}}\right)\right)\rho DU_{\mathrm{C}}^2 \end{aligned} \tag{7}$$

where $\bar{C}_{\mathrm{D}}$ is the average drag force coefficient, C_{D}' is the pulsatory drag force coefficient, C_{L} is the lift

force coefficient, ϕ_D and ϕ_L are phase angles by which drag and lift forces lead the cross-flow displacement of the tether. Their values are determeined through experiment and when the reduced velocity Vr ($Vr=U_C/fD$, f is the natural frequency of tether) is equal to 6.0, ϕ_D and ϕ_L is 130^0 and 50^0 respectively (Srapkaya 2004). The influence of the average drag force f_D is ignored because it changes the equilibrium position of the tether but does not alter the amplitude of VIV. In the present study the coefficient C'_D and C_L are assumed to be constants, i.e. $C'_D = 0.2$ and $C_L = 1.2$ (Ge et al. 2007).

The changes in tether tension consists of two-fold. First, the tunnel oscillation changes the axial tension in the tether, which is defined as parametric excitation and the change can be given by $-T'\cos\omega t$, where T' is the time-varying tension force amplitude, ω is the angular frequency of the oscillation of tunnel. Second, the deflection of tether also changes the axial tension force. Therefore, the total tension force T can be written as

$$T = T_0 - T'\cos\omega t + \frac{1}{2}\frac{EA}{L}\int_0^L\left[\left(\frac{\partial x}{\partial z}\right)^2+\left(\frac{\partial y}{\partial z}\right)^2\right]\mathrm{d}z \quad (8)$$

where T_0 is the initial tension in the tether.

The boundary conditions are specified as follows

$$\begin{aligned} &x(0,t)=x''(0,t)=x''(L,t)=0,\ \ x(L,t)=-x_0\sin\omega t \\ &y(0,t)=y(L,t)=y''(0,t)=y''(L,t)=0 \end{aligned} \quad (9)$$

Here, the prime denotes a derivative with respect to z. The tether is pin-jointed at two ends. In addition, the tip of tether is taken to move together with tunnel and the term $x_0\sin\omega t$ in Equation (9) represents the corresponding boundary condition which is the forcing excitation for the tether vibration just shown as Figure 3.

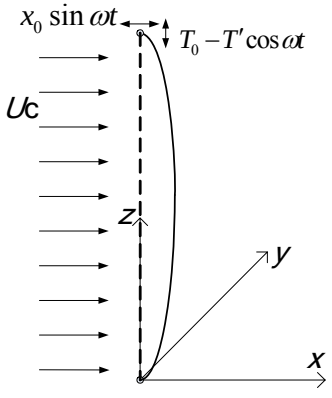

Figure 3. Boundary conditions of a vibrating tether.

3 RESLUTS AND DISCUSSION

Equation (1) is discretized using a second-order central difference method. The length of discretized element Δz is equal to 0.1m. Meanwhile, if the time step Δt is smaller than 10^{-5} s, the solution is convergent. Numerical results are illustrated using the tether with the basic data as presented in Table 1 (Pigorini 1988).

Table 1. Characteristics of tether

Length	100 m
Outer diameter	1.1176 m
Thickness	0.038 m
Dry mass	1000 kg/m
Added mass	1006 kg/m
Bending stiffness	3.854×10^9 N.m^2
Pre-tension	14186 kN

3.1 Natural frequency of the tether

Initially, an attempt was made to determine the vibration frequency of tether without the external fluid force. For this, Equation (1) is rewritten as

$$\overline{m}\frac{\partial^2\mathbf{r}}{\partial t^2}+(C+C')\frac{\partial\mathbf{r}}{\partial t}+EI\frac{\partial^4\mathbf{r}}{\partial z^4}-T\frac{\partial^2\mathbf{r}}{\partial z^2}=0 \quad (10)$$

Here displacement vector is $\mathbf{r}=x+iy$. In the derivation of Equation (10), $\mathbf{r}$ is written as

$$\mathbf{r}(z,t)=\sum_{j=1}^{n}\phi_j(z)\overline{r}_j(t) \quad (11)$$

where $\phi_j(z)$ is the mode-shape function satisfying the tether boundary conditions. For a tether with pinned ends, the mode-shape function is hence given by

$$\phi_j(z)=\sin\frac{j\pi z}{L} \qquad j=1,\cdots\cdots,n \quad (12)$$

where L is the length of tether. Substituting Equations (11) and (12) into Equation (10) and using orthogonality of the mode-shape function, we have

$$\ddot{\overline{r}}_i+2\varsigma_i\omega_i\dot{\overline{r}}_i+\omega_i^2\overline{r}_i=0 \quad (13)$$

Here,

$$\varsigma_i=\frac{C+C'}{2\overline{m}\omega_i}, \quad i=1,\cdots\cdots,n \quad (14)$$

where ω_i is the ith natural frequency of tether and can be expressed by

$$\omega_i=2\pi f_i=\frac{i\pi}{L}\sqrt{\frac{EI}{\overline{m}}\left(\frac{i\pi}{L}\right)^2+\frac{T}{\overline{m}}} \quad (15)$$

Some features of tether dynamics can be illustrated by inspecting its natural frequencies and mode-shapes. The natural frequency as a function of mode number i for the tether is shown in Figure 4. Values for a tensioned string and an untensioned beam with equal length L and mass per unit length

m_s are also shown. The tensioned string and untensioned beam both have the pinned ends, which are the same with the tether. Therefore the formulations of their natural frequencies are written as

$$\begin{aligned} &\text{untentioned beam} && f_{i,\text{beam}} = \frac{i^2\pi}{2}\sqrt{\frac{EI}{\bar{m}L^4}} \\ &\text{tensioned string} && f_{i,\text{string}} = \frac{i}{2}\sqrt{\frac{T}{\bar{m}L^2}} \end{aligned} \quad (16)$$

In this case the natural frequency of tether is seen to follow an untensioned beam with pinned ends. It means that the bending stiffness is dominant for the tether deflection comparing with the axial tension force.

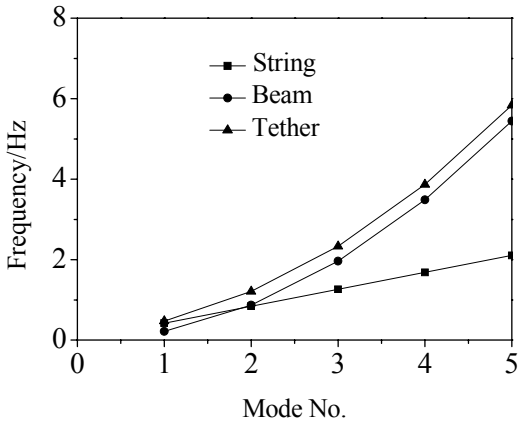

Figure 4. Estimates of natural frequencies for tether, string and beam.

3.2 Dynamic responses of the tether

First, linear model is used to determine the effect of the nonlinearity on the dynamic response of tether. The dynamic formulation for linear model is the same as Equation (1), but the expressions of tension force *T* and external fluid force *F* are different. For simplicity, it is assumed that the tunnel is stationary and the axial tension force in the tether is constant. The coupling effect of hydrodynamic forces between in-line and cross-flow vibrations is also omitted and the right hand side of Equation (1) is expressed as

$$\begin{cases} F_x = f_D + f_D' \\ F_y = f_L \end{cases} \quad (17)$$

Vibrations associated with the first natural frequency are investigated and compared. The current velocity U_C is determined with the Strouhal law

$$U_C = \frac{\omega_i D}{2\pi St} \quad (18)$$

where the vortex-shedding frequency is equal to the chosen natural frequency of the tether ω_i. Thus, the lock-in condition can be imposed automatically. The Strouhal number is chosen to be 0.2 and is the same for both models.

Figure 5(a) presents the two-dimensional motion of the tether mid-span. It is clear that the cross-flow vibration is dominant compared with the in-line vibration. For nonlinear model, shown as Figure 5(b), the trajectory of the tether mid-span is in the shape of '8' that bends towards the upstream direction. Moreover it is seen that the cross-flow amplitude decreases while the in-line amplitude increases. It means that the nonlinearity of tether plays an important role when the vibrations occur due to the current.

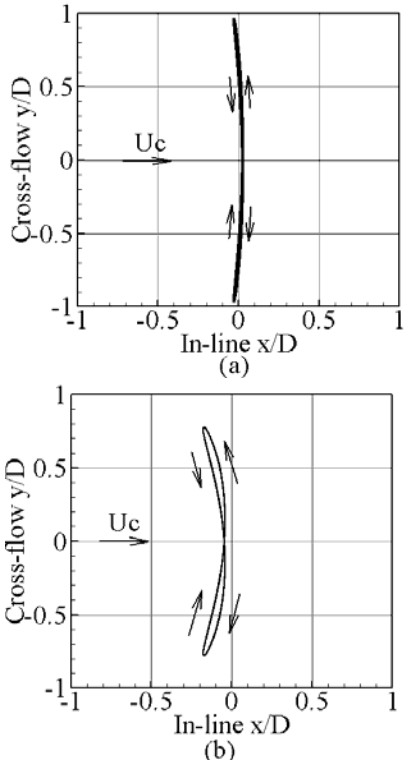

Figure 5. Two−dimensional motion of tether mid-span for $Vr = 6.0$: (a) Linear model, and (b) Nonlinear model.

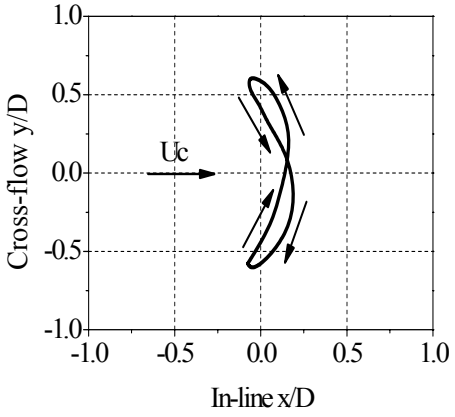

Figure 6. Measured two-dimensional motion of a spring supported cylinder for $Vr = 5.69$ (Wu, 1989).

For verification of the above numerical results,

Figure 6 presents the experimental measurement for a spring supported cylinder (Wu 1989). Comparing with Figure 5(b), one may see that the trajectories of the tether and spring supported cylinder are similar. In experiment, due to the existing of fluid drag force f_{D}, the equilibrium position of VIV moves towards the downstream direction.

Next, in order to analyse the effect of tunnel oscillation on VIV of the tether, it is assumed that the tunnel periodcally oscillates under the linear wave forces. The period of oscillation equals to the surface wave period with the value of 15s. The amplitude of the oscillation of tunnel x_0 can reach 5 meters corresponding to the maximum wave height being 18m (Kanie et al. 1994). Therefore, $x_0/D = 4.47$ and $T'/T_0 = 0.60$ are used here as the strengths of forcing excitation and parametric excitation, respectively. Under such conditions, the response of tether is obtained at mid-span as shown in Figure 7.

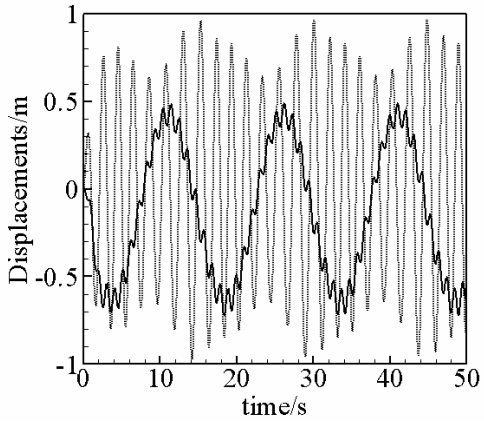

Figure 7. Time history of vibration at tether mid-span with tunnel being vibration, where solid line representing in-line vibration and dotted line representing cross-flow vibration.

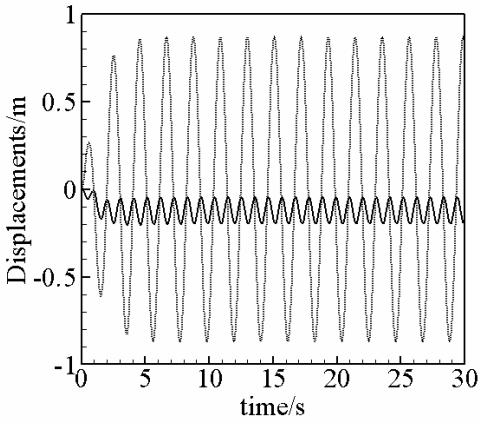

Figure 8. Time history of vibration at tether mid-span with tunnel being stationary, where solid line representing in-line vibration and dotted line representing cross-flow vibration.

If the tunnel is stationary i.e. $x_0 = 0$ and $T' = 0$, the response of the tether mid-span is presented in Figure 8. Comparing with Figure 7, One can see that under the condition of the tunnel oscillation, the amplitude of in-line vibration increases obviously and the corresponding frequency changes from the double vortex-shedding frequency $2\omega_{\mathrm{s}}$ to the surface wave frequency, which is shown as Figures 9(a) and 9(c). In cross-flow, although the maximum amplitude is similar in both cases, the vibration frequency changes, as shown in Figures 9(b) and 9(d), from single peak to multi-peaks. This also leads to the periodical variation of the amplitude for cross-flow vibration.

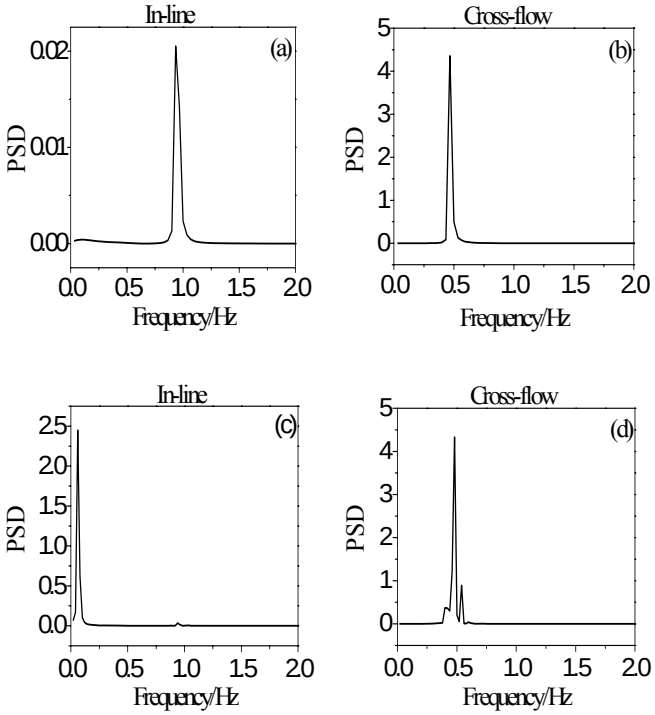

Figure 9. Frequency of vibration obtained at tether mid-span, (a)(b) for tunnel being stationary, and (c)(d) for tunnel being vibration.

4 CONCLUDING REMARKS

A VIV model is presented for predicting the nonlinear dynamic response of submerged floating tunnel tethers which are subjected to current. The nonlinearity of tether plays an important role during the vibration and leads to the increasment of the in-line amplitude while the cross-flow amplitude decreases compared with the linear model. The trajectory of the tether cross-section is in the shape of '8' bending towards the upstream direction, which is similar to the experimental results. The influence of the tunnel oscillation is also considered by introducing the forcing and parametric excitations into the tether model. The amplitudes and frequencies are changed for both in-line and cross-flow vibrations, which means that the influence of tunnel oscillation must be considered in the study of tether VIV.

ACKNOWLEDGMENT

This work is financially supported by National Natural Science Foundation of China (Grant no.10532070), Knowledge Innovation Program of Chinese Academy of Sciences (Grant no. KJCX2-YW-L07) and the LNM initial funding for young investigators.

REFERENCES

Ahrens, D. (1997) *Submerged Floating Tunnels---- A Concept Whose Time Has Arrived. Tunneling and Underground Space Technology, 1997, 12: 317-336.*

Brancaleoni, F., Castellani, A. and D'Asdia, P. (1989) *The Response of Submerged Tunnels to Their Environment. Engineering Structures, 1989, 11: 47-56.*

Facchinetti, M. L., de Langre, E., Biolley, F. (2004) *Coupling of structure and wake oxcillator in vortex-induced vibrations. Journal of Fluids and Structure, 2004, 19:123-140*.

Ge, F., Hui, L. and Hong, Y. (2007) *Vortex induced nonlinear vibrations of submerged floating tunnel tethers. China Journal of Highway and Transport, 2007, 20: 85-89.*

Huang，G., Wu, Y. and Hong Y. (2002) *Transportation of Crossing Waterways via Archimedes Bridge. Ship Building of China, 2002, 43 (supplement): 13-18.*

Kanie, S., Kokubun, H., Mizutani, Y., Mikami, T., Kakuta, Y. (1994) *Analytical Study on Dynamic Response of Submerged Floating Tunnels due to Wave Force. Proc. of the 3rd Symposium on Strait Crossings, Symposium on Strait Crossings: 659-666, Alesund 1994.* Balkema.

Kunisu, H., Mizuno, S., Mizuno, Y., Saeki, H. (1994) *Study on Submerged Floating Tunnel Characteristics under the Wave Condition. Proc. of the 4th International Offshore and Polar Engineering Conference: 27~32, Osaka 1994*, ISOPE.

Mai, J., Luo, Z. and Guan, B. (2004) *Vortex-Induced Dynamic Response of Tension Legs for Submerged Floating Tunnel under Current Effect. Journal of Southwest Jiaotong University, 2004, 39: 600-604.*

Pigorini, B. (1988) *Submerged Tunnels for a Fixed Link across the Strait of Messina. Proc. of the International Congress on Tunnels and Water: 13-31, Madrid 1988.* Balkema.

Remseth, S., Leira, B. J., Okstad, K. M., Mathisen, K. M., Haukas, T. (1999) *Dynamic Response and Fluid/Structure Interaction of Submerged Floating Tunnels. Computers and Structures, 1999, 72: 659-685.*

Srapkaya, T. (2004) *A critical review of the intrinsic nature of vortex-induced vibrations. Journal of Fluids and Structure, 2004, 19: 389-447.*

Wang, X. Q., So, R.M.C. and Chan, K.T. (2003) *A Non‐linear Fluid Force Model for Vortex‐Induced Vibration of an Elastic Cylinder. Journal of Sound and Vibration, 2003, 260: 287‐305.*

Wu, Z. J. (1989) *Current Induced Vibrations of a Flexible Cylinder. The University of Trondheim, 1989*, Norway.